DOI: 10.1002/anie.201105276

Perovskite Phases

$BaFeO_3$: A Ferromagnetic Iron Oxide**

Naoaki Hayashi, Takafumi Yamamoto, Hiroshi Kageyama, Masakazu Nishi, Yoshitaka Watanabe, Takateru Kawakami, Yoshitaka Matsushita, Atsushi Fujimori, and Mikio Takano*

A small class of oxides that contain iron in a high valence state of Fe^{4+} (d^4) are known. The most representative phase is $SrFeO_3$ (SFO) that crystallizes in the cubic perovskite structure containing corner-sharing $(FeO_6)^{12-}$ octahedra and Sr^{2+} ions that occupy the resulting large open voids. It has been shown that SFO and related oxides behave very differently from Fe^{2+} and Fe^{3+} oxides such as FeO, $Fe^{2+/3+}{}_3O_4$, and $LaFe^{3+}O_3$ (LFO). To the best of our knowledge, all these Fe^{2+} and Fe^{3+} oxides are antiferromagnetic (or ferrimagnetic) insulators in their ground states. Valence mixing often generates good electrical conductivity, but even for the most well-known case of Fe_3O_4, an insulating gap of 0.11 eV[1] eventually opens at 119 K (the Verwey transition). Fe_3O_4 and $Y_3Fe^{3+}{}_5O_{12}$ have nontrivial spontaneous magnetizations of approximately 1 μ_B per Fe ion, but these values are due to simple imbalance between the antiferromagnetic sublattices and not to ferromagnetism. In contrast, the Fe^{4+} oxides commonly exhibit a shift toward metallicity and ferromagnetism. SFO maintains cubic symmetry down to low temperatures in spite of the instability inherent to the twofold orbitally degenerate $t_{2g}{}^3e_g{}^1$ configuration and, at the same time, maintains metallic conductivity down to low temperatures.[2,3] SFO is seemingly an antiferromagnet ($T_N \approx 134$ K), but the nearest neighboring spins make an angle of only approximately 46° (3.1 μ_B per Fe ion at 4 K) in the helicoidal spin structure with a long wavelength.[4,5] Moreover, genuine ferromagnetism appears when the specific volume is compressed to $V(7\text{ GPa})/V(0\text{ GPa}) = 0.95$.[6]

As discussed in our recent report on an Fe^{4+} oxide $SrCu^{2+}{}_3Fe^{4+}{}_4O_{12}$,[7] the specificity of Fe^{4+} oxides can be assigned to the fact that the approximate effective charge transfer energy Δ_{eff} drastically drops from 8 eV for FeO and 5.5 eV for LFO to −3 eV for SFO. Thus, $Fe^{3+}(O_6)^{11-}$ or $Fe^{3+}\underline{L}$ ($\underline{L}$: ligand hole) is the realistic picture rather than $Fe^{4+}(O_6)^{12-}$.[8,9] The aforementioned characteristics of "Fe^{4+}" oxides should thus be considered to result from interplay of Fe d electrons and O p holes.[10]

Oxygen-stoichiometric SFO and $CaFeO_3$ (CFO) have been obtained by applying high oxygen pressures of 30 MPa–2 GPa at elevated temperatures (typically ca. 1300 K) to easily obtainable oxygen-deficient phases $SrFeO_{3-\delta}$ and $CaFeO_{2.5}$.[2,3,11] On the other hand, it has been known that $BaFeO_{3-\delta}$ ($\delta \approx 0.1$) prepared in a similar way crystallizes in the 6H or 12H perovskite structure where not only corner-sharing but also face-sharing Fe–O octahedra are contained (Figure 1).[12] However, by using the following process (see the Experimental Section for details), we succeeded in obtaining fully oxidized $BaFeO_3$ (BFO), which crystallizes in the normal perovskite structure. The starting material was a powder of the easily obtained oxygen-deficient 6H phase. The undesirable face-sharing configuration was eliminated by reducing $BaFeO_{2.5}$ before oxidation. In the constituent FeO_6 octahedra of $BaFeO_{2.5}$, FeO_5 pyramids and FeO_4 tetrahedra are connected only by corner sharing.[13] The powder was subsequently oxidized topochemically at low temperatures by using ozone as an oxidant. Ozone is usually considered to be suitable for strong superficial oxidation such as overlayering of silver metal with AgO.[14] Oxidation to Fe^{4+}, Co^{4+}, and Cu^{3+} by ozone has also been limited to the cases of thin films (ca. 50 nm) of SFO, CFO, $SrCoO_3$,[10] and $Ba_2CuO_{3+\delta}$.[15] However, we show below that the $BaFeO_{2.5}$ powder approximately 1 μm in diameter could be oxidized completely by this oxidant.

Figure 2 a shows the room-temperature synchrotron X-ray diffraction (XRD) pattern, which suggests a cubic cell of $a \approx 3.97$ Å. The sharpness of the signals indicates that the

[*] Dr. N. Hayashi
Micro/Nano Fabrication Hub
Center for the Promotion of Interdisciplinary Education and Research, Kyoto University
Yoshida-Honmachi, Sakyo, Kyoto 606-8501 (Japan)
E-mail: hayashi@sou.mbox.media.kyoto-u.ac.jp
T. Yamamoto, Prof. Dr. H. Kageyama
Graduate School of Engineering, Kyoto University
Kyoto 615-8510 (Japan)
Dr. M. Nishi
Institute for Solid State Physics, University of Tokyo
Chiba 277-8581 (Japan)
Y. Watanabe, Prof. Dr. T. Kawakami
Institute of Quantum Science, Nihon University
Tokyo 101-8308 (Japan)
Dr. Y. Matsushita
Beamline BL15XU, SPring-8, NIMS-branch office
Hyogo 679-5148 (Japan)
Prof. Dr. A. Fujimori
Department of Physics, Graduate School of Science
University of Tokyo, Tokyo 113-0033 (Japan)
Prof. Dr. M. Takano
Institute for Integrated Cell-Material Sciences
Kyoto University, Kyoto 606-8501 (Japan)

[**] This study was by a Grant-in-Aid for Scientific Research 20750050, 20750046, 22245009, and 17105002 from the Ministry of Education, Science, Sports and Culture (Japan), and by the Nippon Sheet Glass Foundation for Material Science and Engineering (Japan). We thank Y. Shimakawa of ICR, Kyoto University for allowing the use of the magnetometer, Dr. K. Ohoyama of Tohoku University for his help in the ND measurements, M. Tanaka, and Y. Katsuya of NIMS for their help in the high-resolution synchrotron XRD measurements, and Prof. T. Tohyama of YITP, Kyoto University for useful discussions.

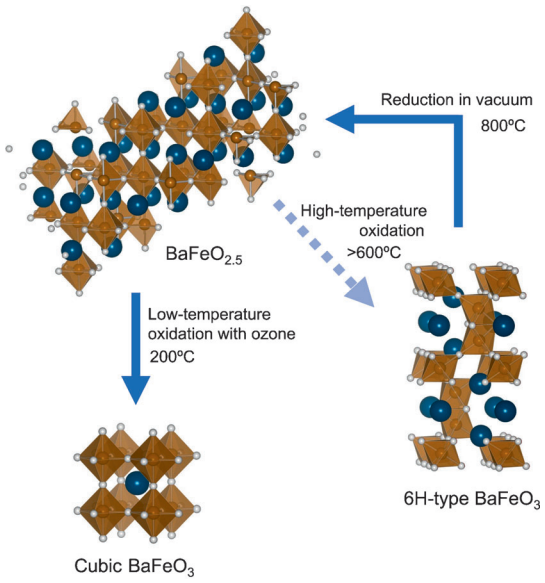

Figure 1. Synthetic route for cubic $BaFeO_3$. Ba Blue, Fe brown, O white.

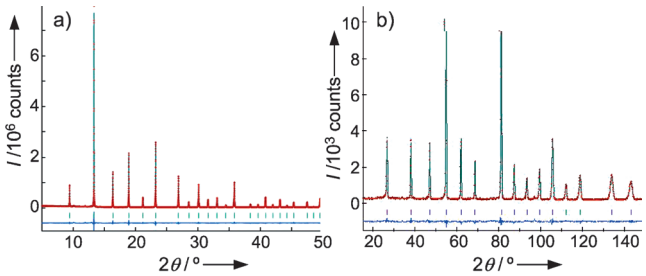

Figure 2. Synchrotron powder XRD profile taken at room temperature (a) and the powder ND profile taken at 150 K (b) for $BaFeO_3$. The overlying crosses and solid lines represent the observed and calculated intensities, respectively. The solid line at the bottom of the spectrum represents the difference between the observed intensity and the calculated intensity. The ticks indicate the calculated peak positions.

powder is well-crystallized and chemically homogeneous, and also that the powder remains stable. The Rietveld refinement, assuming cubic perovskite structure ($Pm\bar{3}m$) as an initial model, quickly converged to small R factors with reasonable magnitudes of temperature factor (B; Figure 2a and Table 1). Essentially the same conclusion was obtained from powder neutron diffraction (ND) measurements (Figure 2b and Table 1). It was also confirmed that the cubic symmetry is preserved to at least 8 K. Since neutrons are sensitive to oxygen, we checked the oxygen content by analyzing the ND data; when allowed to vary, the oxygen site occupancy factor converged to 0.994(7). We thus conclude that BFO is a cubic perovskite that is fully oxidized within experimental error. The Mössbauer spectrum collected at room temperature (Figure 3a) is consistent with this conclusion and consists of a sharp singlet signal with a center shift (CS) of 0.146 mm s^{-1}.

Table 1: Structural parameters for $BaFeO_3$.[a]

Atom	Site	x	y	z	B [Å^2] (XRD, RT)	B [Å^2] (ND, 150 K)
Ba	1*a*	0	0	0	0.247(5)	0.19(5)
Fe	1*b*	1/2	1/2	1/2	0.492(10)	0.36(3)
O	3*c*	1/2	1/2	0	0.73(3)	0.72(4)

[a] $Pm\bar{3}m$ (no. 221), $a = 3.97106(1)$ Å. $R_{wp} = 7.01\%$, $R_I = 1.46\%$, $R_e = 0.42\%$, $R_F = 1.34\%$, $R_p = 4.75\%$ for synchrotron XRD at room temperature, and $a = 3.95435(8)$ Å. $R_{wp} = 6.11\%$, $R_I = 2.58\%$, $R_e = 4.62\%$, $R_F = 1.37\%$, $R_p = 4.80\%$ for ND at 150 K.

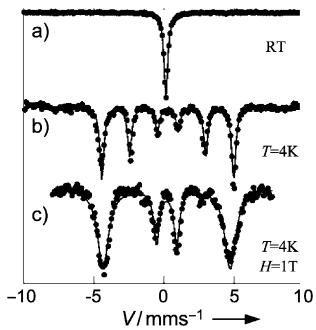

Figure 3. Mössbauer spectra of $BaFeO_3$ taken at room temperature (a) and 4 K (b). The spectrum (c) was obtained from a sample enriched with ^{57}Fe at 4 K in an external field of 1 T applied parallel to the γ-ray beam. The peaks of this spectrum are broadened because of the saturation effect arising from the enrichment. Dotted lines: experimental data points, solid lines: best-fit curves.

Mössbauer measurements also provided firm evidence of magnetic order. A single magnetically split sextet with a hyperfine field (HF) of 22.1 T and 29.1 T appears at 77 K (not shown) and 4 K (Figure 3b), respectively. Interestingly, application of an external field (H) of 0.5 T and above along the γ-ray beam changed the relative peak intensity from the normal 3:2:1:1:2:3 to the 3:0:1:1:0:3 pattern (Figure 3c) and, at the same time, the HF value decreased by the value of H. These results clearly indicate the ferromagnetism of BFO. Consistent with this observation, the magnetization (M) measured at $H = 0.1$ T on cooling showed a pronounced increase followed by saturation at around 120 K (Figure 4a).

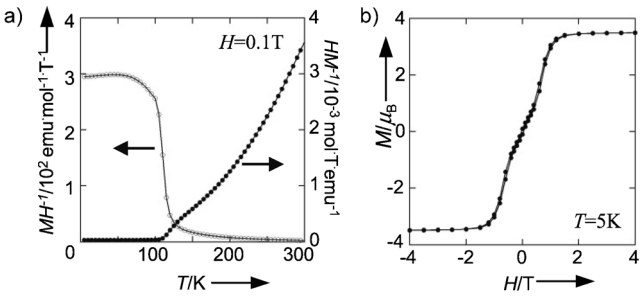

Figure 4. Temperature dependence of magnetization divided by field M/H, and its inverse measured at $H = 0.1$ T on cooling (a) and the M–H curve recorded at 5 K (b).

We have estimated the transition temperature to be 111 K, where the temperature derivative of magnetization shows an anomalous change. The M–H curve (Figure 4b), however, was complex and consisted of a low-field linear part that changed to a high-field ferromagnetic part at approximately

0.3 T at 5 K (ca. 0.2 T at 77 K). A field-induced switching from antiferromagnetism to ferromagnetism was thus suggested. The saturation magnetization corresponds to a large atomic moment of 3.5 μ_B per Fe ion (3.2 μ_B per Fe ion at 77 K), which is consistent with the $Fe^{3+}L$ picture with $S=2$. The usual Curie–Weiss estimation of the atomic moment in the paramagnetic temperature region failed because the curve of $(M/H)^{-1}$ versus T curve has a nonlinear, concave shape (Figure 4a). SFO also behaves similarly although the reason for this is not clear.[4]

The spin state at zero field was examined by ND measurements. Figure 5a shows the profile around the 100 and 110 reflections between 8 K and 303 K, where weak

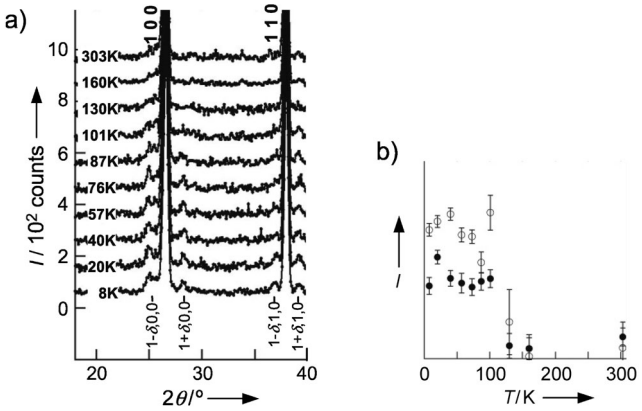

Figure 5. ND profiles showing satellites in the vicinity of the (100) and (110) peaks (a). Temperature dependences of relative intensity for $1+\delta,0,0$ (solid circles) and $1+\delta,1,0$ (open circles) satellite peaks (b).

satellite reflections that indicate the formation of a superstructure with a propagation vector of $\boldsymbol{q}/\boldsymbol{a}^* = [0.06,0,0]$ can clearly be seen. As shown in Figure 5b, these peaks disappear at around 110 K, which is close to the temperature of the magnetic transition. On the other hand, the synchrotron XRD pattern at 80 K did not show these additional signals. We thus conclude that BFO is an antiferromagnet with a spiral spin structure of the A type ($\boldsymbol{q}//\boldsymbol{a}$) that shows a field-induced transition to ferromagnetism at approximately 0.3 T at 5 K (0.2 T at 77 K).

The spiral spin order of BFO is somewhat different from that of SFO, as SFO has its propagation vector along the ⟨111⟩ axis, and the Fe (111) layers rotate their spin axis by approximately 46° from one layer to another. For BFO, however, the propagation vector is along the ⟨100⟩ direction and the Fe (100) layers rotate the yz component of their spin axis by approximately 22° from one layer to another. In this respect it may be concluded that BFO is closer to ferromagnetism than SFO. We believe that BFO must "show metallic properties" better but could not confirm it experimentally because well-sintered pellets could not be produced.

The proper screw spin structure of SFO was classically explained based on the RKKY interaction model featuring a ferromagnetic nearest-neighbor interaction ($J_1 = 1.2$ meV) and antiferromagnetic second-nearest and fourth-nearest neighbor interactions ($J_2 = -0.1$ meV, $J_4 = -0.3$ meV).[5] More recently, Mostovoy[16] proposed another theoretical framework and constructed a phase diagram including various spin structures. The study starts from the ferromagnetic Kondo lattice model involving itinerant electrons of Fe e_g parentage in strongly hybridized d_γ–p_σ orbitals and also localized, spin-polarized t_{2g} electrons. The theoretical consideration was made in terms of p–d charge transfer energy Δ, p–d transfer integral ($pd\sigma$), p–p transfer integral t_{pp}, and the superexchange coupling J between the t_{2g} spins. When J is neglected, the ferromagnetic state (FM) and the proper screw spin state with $\boldsymbol{q}//\langle 100\rangle$ (A-HM) dominate the phase diagram spanned by $\Delta/(pd\sigma)$ and $t_{pp}/(pd\sigma)$. When J is taken into account, the A-type antiferromagnetic state (A-AFM) and the proper screw spin state with $\boldsymbol{q}//\langle 111\rangle$ (G-HM) appear in lower $\Delta/(pd\sigma)$ regions below the A-HM state. Because the cubic lattice constant and hence the Fe–O distance r increase on going from SFO ($r = 1.925$ Å) to BFO ($r = 1.985$ Å), the parameters in the model Hamiltonian should change accordingly. According to Harrison's rule,[17] r varies according to $(pd\sigma) \propto 1/r^{3.5}$, $t_{pp} \propto 1/r^2$, and $J \propto (pd\sigma)^4 \propto 1/r^{14}$, while Δ changes much less. Therefore, the most remarkable difference between SFO and BFO is that the J value is reduced roughly by a factor of two owing to the lattice expansion; that is, in the theoretical treatment developed by Mostovoy, the shift from the G-HM structure of SFO to the A-type spiral structure and ferromagnetism of BFO may be ascribed to the weakening of the antiferromagnetic interactions between the t_{2g} cores. It is interesting to note here that both lattice compression under external pressure[6] and lattice expansion by chemical substitution lead SFO to ferromagnetism.

Recently, two research groups independently prepared $BaFeO_{3-\delta}$ films on the $SrTiO_3$ (001) substrate, but the results are controversial.[18–20] One research group claimed that their film was highly insulating and ferromagnetic ($T_C >$ 300 K),[18,19] while the other claimed metallicity and ferromagnetism with $T_C \approx 235$ K.[20] The observed moments were as small as 0.6 μ_B per Fe ion. This diversity indicates the necessity of careful control of film quality. We are now trying to obtain oxygen stoichiometric films based on the present study.

In conclusion, a new cubic Fe^{4+} perovskite, BFO, was prepared by low-temperature oxidation using ozone. This oxide has an A-type spiral spin structure below 111 K, while application of a small external field induces ferromagnetism with a large atomic moment of 3.5 μ_B per Fe ion. BFO is thus the first reported Fe oxide that shows ferromagnetism at ambient pressure. We note that the magnetic transition temperature increases from 111 K to more than 300 K as external pressure of up to 40 GPa is applied; this feature will be reported elsewhere.

Experimental Section

The sample was prepared as follows: appropriate amounts of $Ba(NO_3)_2$ (99.9%) and $Fe(NO_3)_3{\cdot}9H_2O$ (99.9%) were dissolved in distilled water, to which a fivefold excess of citric acid, a onefold excess of propylene glycol, and an ammonia solution were added while stirring. The solution was condensed at 120 °C for 10 h, and the

resulting polymerized solid was heated first at 450 °C for 2 h and then at 800 °C for 5 h in air to obtain a fine powder of 6H-$BaFeO_{3-\delta}$. The powder was converted to $BaFeO_{2.5}$ by heating in a vacuum of approximately 10^{-4} Pa at 800 °C for 5 h. Oxygen-stoichiometric BFO was obtained by heating the $BaFeO_{2.5}$ at 200 °C for 4 h in oxygen-containing ozone (ca. 10 vol %) flowing at a rate of 100 mL min^{-1}. The ozone was generated by using an ozonizer (Ecodesign, ED-OG-R2).

High-resolution synchrotron XRD experiments were performed using a monochromated incident beam ($\lambda = 0.65297$ Å) at the JASRI SPring-8 BLXU15 line, and the obtained profile was analyzed by the Rietveld method using a RIETAN-2000 program.[21] Powder ND experiments were carried out at $\lambda = 1.82646$ Å on a sample powder packed in a vanadium can using the Kinken powder diffractometer, HERMES, installed at JAEA, Tokai. The temperature and field dependence of the magnetization was measured by using a SQUID magnetrometer (Quantum Design, MPMS2) between 5 K and 300 K up to 5 T. ^{57}Fe Mössbauer measurements were performed in transmission geometry using ^{57}Co/Rh as a radiation source and α-Fe as a control for velocity calibration and center shift. The collected spectra were computer-fitted using the Lorenzian function.

Received: July 27, 2011
Published online: November 7, 2011

Keywords: charge transfer · iron · magnetic properties · ozone · perovskite phases

[1] U. Buchenau, I. Müller, *Solid State Commun.* **1972**, *11*, 1291 – 1293.
[2] J. B. MacChesney, R. C. Sherwood, J. F. Potter, *J. Chem. Phys.* **1965**, *43*, 1907 – 1913.
[3] T. Takeda, R. Kanno, Y. Kawamoto, M. Takano, S. Kawasaki, T. Kamiyama, F. Izumi, *Solid State Sci.* **2000**, *2*, 673 – 687.
[4] T. Takeda, Y. Yamaguchi, N. Watanabe, *J. Phys. Soc. Jpn.* **1972**, *33*, 967 – 969.
[5] T. Takeda, S. Komura, N. Watanabe, Ferrites, Proceedings of the Third International Conference of Ferrites (ICF3), Kyoto, **1980**, pp. 385 – 388.
[6] T. Kawakami, S. Nasu, *J. Phys. Condens. Matter* **2005**, *17*, S789 – 793.
[7] I. Yamada, K. Tsuchida, K. Ohgushi, N. Hayashi, J. Kim, N. Tsuji, R. Takahashi, M. Matsushita, N. Nishiyama, T. Inoue, T. Irifune, K. Kato, M. Takata, M. Takano, *Angew. Chem.* **2011**, *123*, 6709 – 6712; *Angew. Chem. Int. Ed.* **2011**, *50*, 6579 – 6582.
[8] A. E. Bocquet, A. Fujimori, T. Mizokawa, T. Saitoh, H. Namatame, S. Suga, N. Kimizuka, Y. Takeda, M. Takano, *Phys. Rev. B* **1992**, *45*, 1561 – 1570.
[9] M. Abbate, F. M. F. de Groot, J. C. Fuggle, A. Fujimori, O. Strebel, F. Lopez, M. Domke, G. Kaindl, G. A. Sawatzky, M. Takano, Y. Takeda, H. Eisaki, S. Uchida, *Phys. Rev. B* **1992**, *46*, 4511 – 4519.
[10] N. Hayashi, T. Terashima, M. Takano, *J. Mater. Chem.* **2001**, *11*, 2235 – 2237.
[11] P. M. Woodward, D. E. Cox, E. Moshopoulou, A. W. Sleight, S. Morimoto, *Phys. Rev. B* **2000**, *62*, 844 – 855.
[12] K. Mori, T. Kamiyama, H. Kobayashi, T. Otomo, K. Nishiyama, M. Sugiyama, K. Itoh, T. Fukunaga, S. Ikeda, *J. Appl. Cryst.* **2007**, *40*, s501 – s505, and references therein.
[13] M. Parras, M. Vallet-Regí, J. M. González-Calbet, M. A. Alario-Franco, J. C. Grenier, P. Hagenmuller, *Mater. Res. Bull.* **1987**, *22*, 1413 – 1419.
[14] R. O. Suzuki, T. Ogawa, K. Ono, *J. Am. Ceram. Soc.* **1999**, *82*, 2033 – 2038.
[15] H. Yamamoto, M. Naito, H. Sato, *Jpn. J. Appl. Phys.* **1997**, *36*, L341 – L344.
[16] M. Mostovoy, *Phys. Rev. Lett.* **2005**, *94*, 137205.
[17] W. A. Harrison, *Electronic Structure and the Properties of Solids*, Dover, New York, **1989**.
[18] T. Matsui, H. Tanaka, N. Fujimura, T. Ito, H. Mabuchi, K. Morii, *Appl. Phys. Lett.* **2002**, *81*, 2764 – 2766.
[19] E. Taketani, T. Matsui, N. Fujimura, K. Morii, *IEEE Trans. Magn.* **2004**, *40*, 2736 – 2738.
[20] C. Callender, D. P. Norton, R. Das, A. F. Hebard, J. D. Budai, *Appl. Phys. Lett.* **2008**, *92*, 012514.
[21] F. Izumi, T. Ikeda, *Mater. Sci. Forum* **2000**, *321 – 324*, 198 – 203.

